Determination of Pore Sizes and Volumes of Porous Materials by ^{129}Xe NMR of Xenon Gas Dissolved in a Medium

Ville-Veikko Telkki, Juhani Lounila, and Jukka Jokisaari*

NMR Research Group, Department of Physical Sciences, University of Oulu, P.O. Box 3000, FIN-90014 University of Oulu, Finland

Received: September 7, 2005; In Final Form: October 27, 2005

In our previous paper (*J. Phys. Chem. B* **2005**, *109*, 757) it was illustrated that the ^{129}Xe NMR spectra of xenon dissolved in acetonitrile confined into mesoporous materials give detailed information on the system, especially about the pore sizes. A resonance signal originating from xenon atoms sited in very small cavities built up inside the pores during the freezing transition (referred to as signal D) turned out to be highly sensitive to the pore size. The emergence of this signal reveals the phase transition temperature of acetonitrile inside the pores, which can also be used to determine the size of the pores. In addition, the difference in the chemical shifts of two other signals arising from xenon dissolved in bulk and confined acetonitrile (B and C) provides another method for determining the pore sizes. In the present work, the observed correlations have been investigated using an extensive set of measurements with a variety of porous materials (silica gels and controlled pore glasses) with the mean pore diameters ranging from 43 to 2917 Å. The usefulness of the correlations has been demonstrated by calculating the pore size distributions from the spectral data. The distributions are in agreement with those reported by the manufacturers, when the mean pore diameter is smaller than ∼500 Å. In addition, it has been shown that the porosity of the materials can be determined by comparing the intensities of the signals arising from the bulk and confined liquid. When acetonitrile is replaced by cyclohexane in the sample, the dependence of the chemical shift difference between the B and C signals on the pore size becomes more sensitive, but no D signal appears below the freezing point. In addition, the influence of xenon gas on the melting points of bulk and confined acetonitrile has been studied by ^{1}H NMR cryoporometry. The measurements show that the temperature of the latter transition lowers slightly more, and consequently affects the pore sizes calculated by means of the difference in the phase transition temperatures. Hysteresis in the phase transitions in a cooling−warming cycle has also been studied as a function of the temperature stabilization time by ^{129}Xe NMR of xenon dissolved in acetonitrile.

1. Introduction

Porous materials are of great interest in technological and scientific applications as well as in natural processes. For instance, they are used in chemical engineering in heterogeneous catalysis, chromatography, filtering of gases and liquids, and drying of bulk goods. Specific surface area, gas and liquid permeability, total pore volume, and pore tortuosity are examples of important properties of porous materials. Perhaps the most important feature is the *distribution* of pore sizes. Classical methods for pore size determination are the gas adsorption/desorption technique and mercury porosimetry.[1] However, these methods have some serious disadvantages: they are quite time-consuming, the underlying theories contain many approximations, the high pressures required in the mercury porosimetry method may cause changes in the pore structure of the sample, and so forth. Therefore, there have been efforts to develop novel methods. In many applications, particular interest is focused on materials whose pore size is in the *mesoporous* range (diameter between 20 and 500 Å). Thus, an efficient porometer operating in this specific range is required.

We have introduced a novel method (proposed to be referred to as *xenon porometry*) recently, which makes it possible to determine the pore sizes by three different ways.[2] In the method, the porous material is immersed in a liquid, which acts as a medium, and xenon gas is dissolved into the sample. Its atoms act as probes because the nuclear magnetic resonance frequency of the ^{129}Xe isotope (a spin-$^{1}/_{2}$ nucleus) is known to be extremely sensitive to changes of its local environment.[3] We demonstrated that, when acetonitrile is used as the medium, the chemical shift of a particular signal observed below the melting point of the confined medium is highly sensitive to the pore size and its shape is sensitive to the pore radius distribution function. The difference of the chemical shifts of two other signals, which arise from xenon dissolved in bulk and confined medium, is also dependent on the pore size. In addition, we demonstrated that the phase transition points of bulk and confined medium can be deduced from the changes in the chemical shifts and intensities of the signals and from the appearance or disappearance of them. According to the Gibbs−Thompson equation,[4] the melting point depression, ΔT, of a substance confined to a cylindrical pore is inversely proportional to pore radius, R_p

$$\Delta T = T_0 - T = \frac{2\sigma_{sl}T_0}{\Delta H_f \rho_s R_p} \equiv \frac{k_p}{R_p}. \quad (1)$$

Here, T_0 and T are the melting points of the bulk and confined liquid, respectively, σ_{sl} is the surface energy of the solid−liquid interface, ΔH_f is the specific bulk enthalpy of fusion, and ρ_s is the density of the solid. The constant k_p defined in eq 1 is

* Corresponding author. E-mail: jukka.jokisaari@oulu.fi.

10.1021/jp055053n CCC: $30.25
Published on Web 12/03/2005

TABLE 1: Properties of the Used Porous Materials Announced by the Manufacturers

material	mean pore diameter (Å)	width of the pore diameter distribution[b]	specific pore volume (cm^3/g)	specific surface area (m^2/g)	particle size (μm)
silica gel 40	42.7[a]				63−200
silica gel 60	47.5[a]		0.74−0.84	480−540	63−200
silica gel 100	63.8[a]		0.9−1.2	270−370	63−200
CPG 81	81	9	0.49	197	125−177
CPG 128	128	5.1	0.8	141.2	37−74
CPG 237	237	4.3	0.95	78.8	125−177
CPG 375	375	6.8	1.49	95	125−177
CPG 538	538	5.6	1.12	42.9	125−177
CPG 1032	1032	3.7	1.21	27.1	125−177
CPG 2917	2917	6.8	0.9	8.3	125−177

[a] Determined by ^{1}H NMR cryoporometry in this study using CPGs as calibration samples. [b] At least 80% of the pores have a diameter within $D_0(1 \pm X/100)$, where D_0 is the mean pore diameter and X is the number shown in the column.

characteristic of each probe liquid. Consequently, as the phase transition temperatures can be determined, the average pore radius of the sample can be calculated by eq 1 in the same way as in NMR cryoporometry.[5]

In the present study, an extensive set of measurements with a variety of mesoporous materials (controlled pore glasses and silica gels) has been carried out to investigate the above-mentioned correlations and to discern the size ranges where these methods are applicable. It is demonstrated that information about porosity can also be extracted from the ^{129}Xe NMR spectral data. Besides acetonitrile, cyclohexane is used as the medium, and the behavior of cyclohexane in confinement is studied. Finally, the effects of xenon gas on the phase transition temperatures and hysteresis are explored.

2. Experimental Section

Controlled pore glasses (CPGs) and silica gels were delivered by CPG Inc. (Lincoln Park, New Jersey) and Merck (Darmstadt, Germany), respectively. The nominal pore diameters of the CPGs were between 81 and 2917 Å, and those of silica gels were between 40 and 100 Å. The properties of the materials have been listed in Table 1. Our ^{129}Xe NMR measurements showed that the nominal pore diameters announced by the two manufacturers are not quite compatible with each other. Hence, we determined the mean pore diameters of silica gels by NMR cryoporometry[5] using the CPG materials as calibration samples. The resulting value of coefficient k_p in eq 1 for acetonitrile was 478 KÅ. This value is 12% smaller than the value measured earlier by Aksnes et al. (545 KÅ)[6] using less precisely controlled silica materials for calibration. Besides the use of different calibration materials, the discrepancy in k_p may be due partly to the fact that our calibration samples also contain xenon gas. (The influence of xenon on the phase transition temperatures will be discussed later.) The mean pore diameters of silica gels measured by the determined k_p value are considerably smaller than those of the CPGs (see Table 1).

Acetonitrile and cyclohexane were obtained from Fluka (Buchs, Switzerland), and they were used without further purification after drying the liquid over molecular sieves. ^{129}Xe-isotope-enriched (99.95%) xenon gas was delivered by Chemgas (Boulogne, France).

The samples were prepared as follows: First, the powder-like porous material was dried keeping the sample tube in a vacuum line overnight at the temperature of 100 °C. Then, the medium (acetonitrile or cyclohexane) was degassed, and the powder was immersed in excess of medium. After connecting the sample tube to the vacuum line again, about 3.5 atm of xenon gas was added, and the glass tube was sealed with a flame. The outer diameter of the sample tube was 10 mm. In addition, the cyclohexane samples and the older acetonitrile samples also contain an inner xenon thermometer as was described in our previous work.[2]

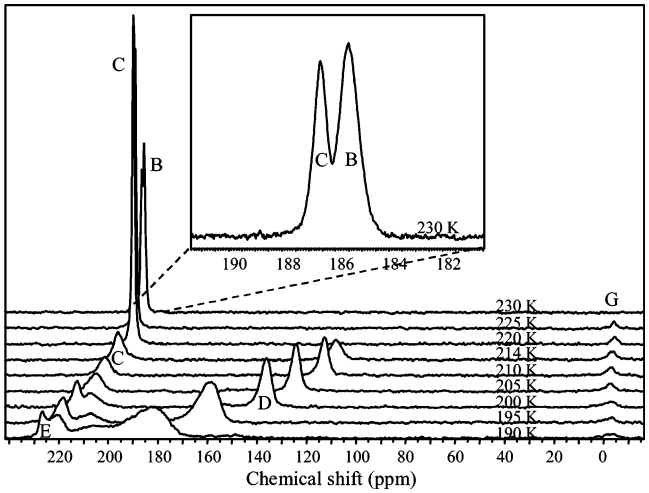

Figure 1. ^{129}Xe NMR spectra of the sample containing CPG 81 in acetonitrile at different temperatures. The measurement temperatures are shown at the spectra. The chemical shift (δ) range of signals B and C at 230 K is shown expanded in the inset.

One-dimensional ^{129}Xe NMR spectra were measured on a Bruker DRX500 spectrometer (resonance frequency 138.3 MHz). The spectra were recorded using a 10-mm high-resolution probehead applying 30° pulses, an 8-s repetition time, and accumulating 100−200 scans. The measurement temperature range was 190−235 K for the samples containing acetonitrile and 204−288 K for the samples containing cyclohexane. The steps of the temperature series were 1−5 K and the temperature was allowed to stabilize 15−20 min after each change. During an experiment, the monitored temperature varied less than ±0.1 K. The spectra were measured from low to high temperatures in order to avoid the supercooling effects of the liquid. The ^{129}Xe resonance signal measured at 230 K for acetonitrile and 290 K for cyclohexane from a bulk xenon gas sample of pressure ~6 atm (fixed to 0 ppm) was used as an external reference in the spectra. In the analysis, the reference has been corrected to correspond to the chemical shift of zero pressure gas. This has been done by using the virial expansion for the dependence of chemical shift of xenon gas on density.[7,8]

3. Acetonitrile as a Medium

3.1. Spectra. Figure 1 displays the ^{129}Xe NMR spectra of the sample containing CPG 81, acetonitrile as a medium, and xenon gas at different temperatures. The signals have been labeled in the figure, and the origins of the components have been analyzed in detail in our earlier work.[2] In summary, signals B and C originate from xenon dissolved in the *liquid* medium. Signal B arises from the bulk medium in the spaces between the particles of porous material and on top of the material. It vanishes below the freezing temperature of the bulk acetonitrile (227 K) because the transition from liquid to solid is accompanied by an abrupt reduction of gas solubility. Signal C originates from liquid *inside* the pores, and it gradually vanishes at lower temperatures, as the confined medium freezes.

Signal D arises from xenon in small pockets appearing inside the pores. The pockets build up during the freezing of the confined medium, as the volume of the medium decreases

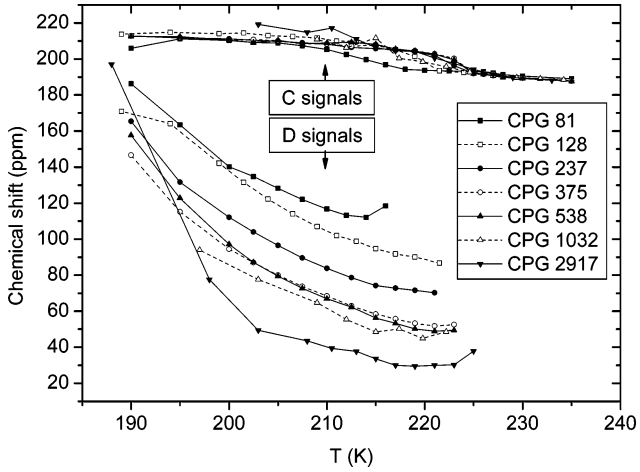

Figure 2. ^{129}Xe chemical shifts of signals C and D as a function of temperature from the samples containing seven different CPG materials in acetonitrile. The lines between the symbols are to guide the eye.

substantially. The signal vanishes as the confined medium melts. Because of the relatively high xenon pressure and capillary condensation, a part of xenon gas in the pockets liquefies at the lowest measurement temperatures. There is a rapid exchange between the gas and liquid sites in the tiny pockets, and the observed chemical shift is the weighted average of the shifts in the gas and liquid sites. Therefore, the chemical shift of signal D changes rapidly at the lowest temperatures.

As the *bulk* acetonitrile freezes, cavities are also formed between the particles of porous materials (because of the volume change) and signal G originates from xenon in there. The cavities are much bigger than those inside the pores so that the chemical shift of signal G is close to that of bulk gas. Signal E (close to 220 ppm) arises from liquefied xenon.

3.2. Chemical Shift of Signal D. Signal D arises from xenon gas inside the pockets formed in the pores during the freezing of the confined medium. The perturbation due to the interaction of a xenon atom with its surroundings increases the chemical shift (or decreases the shielding) of the xenon nucleus. The smaller the pocket is, the stronger the perturbation and the higher the chemical shift of the signal D. Because the size of the pocket depends on the pore size, the chemical shift of signal D is also dependent on the pore size. This is demonstrated by the experimental data in Figure 2.

A simple correlation between the chemical shift of signal D and the pore size was presented in our previous work[2] in which the resonances were measured from three different silica gels with nominal pore diameters of 40, 60, and 100 Å. In the present study, the measurements have been performed in a much wider pore size range (diameters between 43 and 2917 Å) using both silica gels and controlled pore glasses. The mean pore radii of the materials as a function of the chemical shift of signal D have been plotted in Figure 3. The chemical shift values have been determined at 213 K, except for silica gels, in which the melting point of the confined liquid is lower because of the small pore size. In this case, the chemical shift values have been taken from the highest temperature where phase transition effects do not influence the intensity and the chemical shift of signal D. This temperature varies from 210 to 197 K with decreasing average pore size. In principle, the correlation between the chemical shift and pore size could be determined at one single temperature below the melting point of the smallest pores (i.e., 197 K in this case). However, a significant part of xenon in the pockets has liquefied at this temperature. Therefore, the chemical shift of signal D approaches that of liquid xenon in all of the

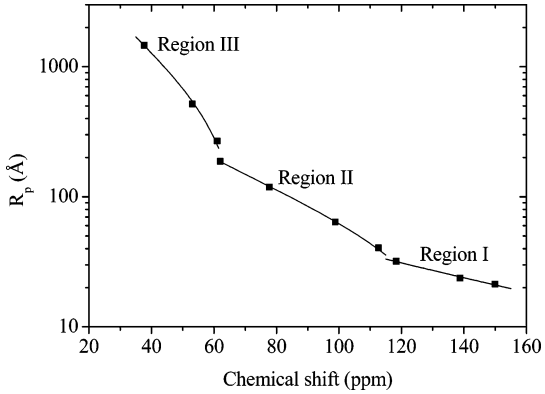

Figure 3. Mean pore radius, R_p, with respect to the chemical shift of signal D measured from the samples containing acetonitrile. The solid lines represent least-squares fit to the experimental points using eq 2.

pores. This decreases the sensitivity of the chemical shift to the pore size.

When the radii are plotted on a logarithmic scale, it can be seen clearly that the figure can be divided into three separate regions. The data points of silica gels constitute the region I. There are three possible reasons why these points deviate from the trend of the CPG materials. First, the measurement temperature is different, as explained above. Second, the geometries of the pores and pore networks inside these two materials are different, and the concept of mean pore radius means slightly different things. Third, there are some uncertainties in the determination of the mean pore radius of silica gels by NMR cryoporometry because it turned out that the experimental data cannot be exactly reproduced by the Gibbs−Thomson equation (eq 1). However, the k_p value has been determined using materials with larger mean pore radii than those of the silica gels. Hence, the evaluation of the pore sizes involves extrapolation, rather than interpolation, of curve 1, which tends to also increase the uncertainty of the results.

Also, the data points measured from the CPG materials divide into two separate groups. These groups appear in regions II and III, where R_p is smaller and larger than about 250 Å. In region III, the line width of signal D is clearly larger than that in region II. The difference of the behavior of signal D from the smaller and larger pores (from regions II and III) may be due to a difference in the shape of the pockets inside these pores. To get a proper explanation for this peculiar phenomenon, further investigations with different media are needed.

The solid lines in Figure 3 show that the dependence of the average pore radius (R_p) on the chemical shift (δ) of signal D can be described in each region by the simple model function

$$R_p = \frac{a}{\delta} - b. \qquad (2)$$

Least-squares adjustments of parameters a and b resulted in the values $a = 6040$ Å/ppm and $b = 19.3$ Å in region I, $a = 20279$ Å/ppm and $b = 140.7$ Å in region II, and $a = 118713$ Å/ppm and $b = 4169$ Å in region III. Note that the parameter values from the data points of the silica gels (region I) differ from the values determined in our previous work.[2] This is due to the fact that in the present study the mean pore radii measured by NMR cryoporometry have been used, instead of the nominal pore radii announced by the manufacturer, and the measurement temperatures were different.

The chemical shift of signal D measured from CPG 2917 is almost 40 ppm, whereas the chemical shift of free gas (corresponding to the D signal from an infinitely large pore) is

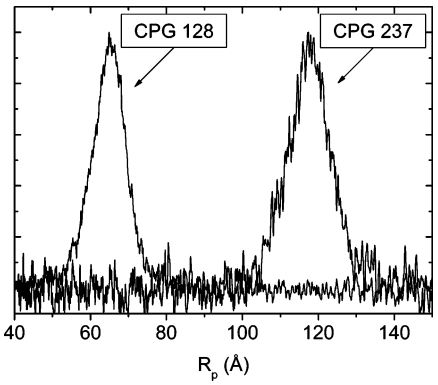

Figure 4. Pore size distributions of CPG 128 and 237 depicted from the shape of signal D and the relation between R_p and δ (eq 2, region II).

close to zero ppm. This, together with the correlation shown in Figure 3, indicates that the chemical shift depends on the pore size even up to micrometer range.

Because there is a one-to-one correspondence between the pore size and the chemical shift, a distribution of pores of different sizes produces a corresponding distribution of signals of different chemical shifts, that is, a characteristic NMR line shape, presuming that the solid matrix of frozen acetonitrile prevents an exchange of xenon atoms between the pockets of different sizes (on the NMR time scale). Therefore, it is possible to extract the pore size distribution function from the shape of signal D. The analysis is particularly simple, if the intrinsic line width of signal D is negligible in comparison with the line width resulting from the pore size distribution. Then the analysis reduces to a conversion of the chemical shift scale of the NMR spectrum to the pore size scale by eq 2. This has been illustrated in Figure 4, where the resulting pore size distributions of two CPG materials with mean pore radii in region II are shown.

The proportion of the half width at half-maximum of the pore size distribution to the center of mass of the distribution is 7.4% for CPG 128 and 4.3% for CPG 237. According to numerical integrations, the area under the distribution curve between the half-maximum points is about 67% of the total area for both materials. Therefore, it can be estimated that 67% of the pores have a radius within $\pm$7.4 and 4.3% of the mean pore radius in the case of CPG 128 and 237, respectively. For comparison, the manufacturer announces that at least 80% of the pores have diameters within $\pm$5.1 and 4.3% of the mean pore diameter for the same materials. The distribution functions shown in Figure 4 are not much broader, indicating that the simple method of analysis neglecting the intrinsic line width of signal D is a reasonable approximation.

The line width of signal D measured in region I from the silica gels increases from 15 to 40 ppm with decreasing mean pore size of the sample, whereas it is about 4 ppm in region II for CPG 81-375. Broader signals from smaller pores are expected because the sensitivity of the chemical shift of signal D to the pore size increases with decreasing pore sizes. In addition, the pore size distributions of the silica gels are known to be wider than those of the CPGs. However, because the data points used in the determination of correlation 2 in region I have been measured at different temperatures, the pore size distributions of materials containing small pores cannot be determined by this correlation from one single spectrum recorded at a single temperature. Another method for the pore size determination for smaller pores will be described in the next section.

The line width of signal D measured in region III is roughly twice as large as that in region II. This is unexpected because the sensitivity of the chemical shift to the pore size decreases with increasing pore size, while the relative width of the pore size distribution function is approximately the same (6% on the average) in both regions. Hence, the line broadening resulting from the pore size distribution actually decreases with increasing pore size. In region III, there must be some effect that substantially increases the *intrinsic* line width of signal D. This masks the effects of the pore size distribution and complicates the determination of the distribution function from the line shape.

There are two types of behavior of signal D around the melting point of the confined acetonitrile. In the case of the smaller pores, the rapid decrease in the intensity of the signal with increasing temperature is accompanied by a sharp rise of its chemical shift. This implies that there is a gradual decrease in the average density of confined acetonitrile during the melting, possibly due to a progressive layer-by-layer melting of the confined nanocrystal.[9] As the volume of acetonitrile increases, the pockets become smaller, and the chemical shift of xenon gas inside them increases, finally approaching that of xenon dissolved in liquid acetonitrile. This phenomenon cannot be seen in bigger pores, where melting is more abrupt. Instead, the shift can even slightly decrease with increasing temperature (see Figure 2). This may be a consequence of the fact that smaller pores inducing higher resonance frequencies melt earlier than the larger ones, and as these frequencies vanish, the center of mass of the signal moves toward lower frequencies. Therefore, it can be concluded that crystals in pores larger than about 100 Å in diameter melt at a single temperature, like bulk crystals, and crystals in smaller pores melt gradually within a finite temperature range, which is observed to be 2$-$9 K in width in these measurements. The gradual melting of small crystals may cause spurious broadening of the pore size distributions determined by the methods that utilize the Gibbs$-$Thompson equation (such as NMR cryoporometry and thermoporosimetry[1]).

3.3. Difference in the Chemical Shifts of Signals B and C. Signals B and C arise from xenon dissolved in a bulk and confined medium, respectively. The slightly higher chemical shift of signal C, as compared to that of signal B, is due to the interactions of xenon atoms with the surface of the pore walls. The interactions take place either directly or through the medium. The smaller the pore is the stronger they are, and thus the chemical shift difference of the signals, $\delta_C - \delta_B = \Delta\delta$, increases with decreasing pore size, as was shown in our previous work with silica gel samples.[2] The results from the present measurements with a wider pore radius range at 235 K and close to room temperature are shown in Figure 5. The relation between $\Delta\delta$ and R_p can be approximated by a model function consisting of two exponential functions

$$R_p = c\exp\left(-\frac{\Delta\delta}{d}\right) + f\exp\left(\frac{\Delta\delta}{g}\right). \quad (3)$$

A least-squares refinement of parameters c, d, f, and g of acetonitrile at 235 K resulted in values $c = 144.4$ Å, $d = 0.5453$ ppm, $f = 21.66$ Å, and $g = 293.8$ ppm. At 300 K, the results were $c = 155.2$ Å, $d = 0.5879$ ppm, $f = 34.15$ Å, and $g = 9.234$ ppm. The shift between signals C and B is seen to increase with increasing temperature. These signals merge together when the pore radius is larger than about 60 Å. Thus, this is the upper limit where the chemical shift difference of them can be utilized for the pore size determination.

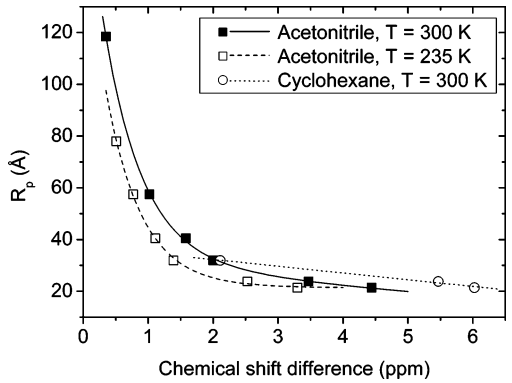

Figure 5. Average radius, R_p, as a function of the chemical shift difference of the ^{129}Xe signals from the confined and bulk liquid (C and B) when acetonitrile and cyclohexane have been used as a medium. The data points have been measured from the silica gels and CPG81, CPG115, CPG156, and CPG237 samples. The measurement temperatures are shown in the figure.

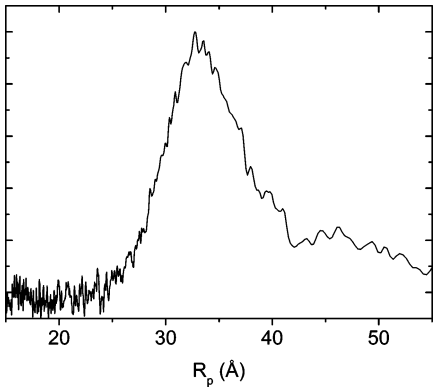

Figure 6. Pore size distribution of silica gel 100 depicted by means of the shape of signal C and the relation between R_p and $\Delta\delta$ at 300 K.

Because of the one-to-one correspondence between the pore radius, R_p, and the chemical shift difference of signals C and B, the line shape of signal C is expected to represent the pore size distribution, like in the case of signal D, if diffusion of xenon is slow enough. The pore size distribution of silica gel 100 has been plotted in Figure 6 by converting the chemical shift scale of signal C to the pore radius scale using eq 3 (i.e., neglecting the intrinsic line width of the signal). The maximum of the distribution is at 33 Å, which is very close to the value of the average pore radius of silica gel 100 (32 Å) used in the calibration of the correlation between R_p and $\Delta\delta$. The half width at half-maximum of the distribution is 4.0 Å, which means that a majority of the pores have radii within ±13% of the mean pore radius. The larger relative width of the resulting distribution as compared to those of CPGs is expected because the pore size distributions of the silica gels are wider than those of CPGs.

The resonance frequency of a xenon atom dissolved into a confined medium is characteristic of a single pore size only on the condition that diffusion is sufficiently slow. To observe two different signals from two sites where the difference of the resonance frequencies of the nuclei is $\Delta\nu$, the lifetime of a spin at one site should be larger than $1/(2\pi\Delta\nu)$,[10] which is referred to as an NMR time scale. If the lifetime is much shorter, then the observed resonance frequency is the weighted average of the frequencies corresponding to each site. As compared to pure xenon gas, the medium slows down the diffusion considerably. At room temperature, the translational diffusion coefficient of bulk xenon gas is 5.3×10^{-6} m^2/s,[11] whereas it is about 2×10^{-9} m^2/s for xenon dissolved in water.[12] Because the full width at half-maximum of signal C measured from acetonitrile confined to silica gel 100 is about 100 Hz, the NMR time scale can be approximated to be 1.6 ms (the line width of signal C varies from ~450 Hz for silica gel 40 to ~75 Hz for CPG 81). Using the diffusion coefficient in bulk water, it can be estimated that the root-mean-square distance traveled by a free xenon atom in one dimension during the NMR time scale is about 2.5 μm. In mesoporous materials, the corresponding distance must be much shorter because the walls of the pores severely hinder the diffusion. Nevertheless, the motion of xenon atoms may lead to some averaging of the frequency over pores of different sizes. This may narrow the pore size distribution function obtained from the shape of signal C.

Comparing the sensitivity of the resonance frequency to the pore size for xenon dissolved in a medium (Figure 5) with that for pure xenon gas,[13] and using the above diffusion coefficients, it can be estimated that the distance traveled by a xenon atom during the NMR time scale is in a medium 2 or 3 orders of magnitude shorter than that in the gas phase. Hence, the motional narrowing of the NMR line is expected to be a much smaller problem for xenon dissolved in a confined medium than for pure xenon gas in porous materials. If it can be neglected, then signal C can be taken to be a convolution of the pore size distribution function in the chemical shift range and the intrinsic line shape function (i.e., the shape of a resonance line observed from pores of a one single size).

Signal B arises mainly from a liquid between the particles of porous materials, and its line width is almost 2 orders of magnitude larger than that of a bulk liquid (~100 Hz). The broadening is due to the surfaces of the porous materials, which change the magnetic field experienced by the xenon nuclei. If there are some macropores in the materials, then they give their own contribution to the resonance distribution of signal B.

3.4. Determination of the Specific Pore Volume. If the solubility of xenon is the same in bulk and confined liquid, then the integrated intensities of signals B and C ($I_B \equiv I_{bulk}$ and $I_C \equiv I_{pore}$) are directly proportional to the volumes of the corresponding phases (V_{bulk} and V_{pore}) so that $V_{bulk}/V_{pore} = I_{bulk}/I_{pore}$. The total volume of the region where the NMR signals are recorded, V_{tot}, is the sum of the volumes of pores (V_{pore}), of the voids between the particles of the porous materials (V_{bulk}), and of the solid skeleton of the porous material (V_{solid})

$$V_{tot} = V_{pore} + V_{bulk} + V_{solid} \tag{4}$$

The volume of the solid can be determined, if the mass of the porous material in the measurement region (m_{solid}) and the density of the solid skeleton (ρ_{solid}) are known ($V_{solid} = m_{solid}/\rho_{solid}$). If V_{tot} is also known, then the porosity of the porous material can be calculated by the following equation:

$$\frac{V_{pore}}{m_{solid}} = \frac{V_{tot} - V_{solid}}{m_{solid}(1 + V_{bulk}/V_{pore})} = \frac{V_{tot}\rho_{solid} - m_{solid}}{m_{solid}\rho_{solid}(1 + I_{bulk}/I_{pore})} \tag{5}$$

Using the integrals of B and C signals measured at 300 K, the porosities of CPG 81 and Silica gel 100 have been calculated by eq 5, and the resulting values are shown in Table 2 together with the data used in the calculations. The results are in good agreement with those determined by the manufacturers; the calculated porosity of silica gel 100 is in the range of the values announced by the manufacturer, and that of CPG 81 is slightly (ca 10%) smaller than the value of the manufacturer.

The intensity ratio I_{bulk}/I_{pore} has been observed to increase slightly with increasing temperature. Because the ratio $V_{bulk}/$

TABLE 2: Porosities and the Values Needed for Its Calculation for Two Different Porous Materials

material	m_{solid} (g)	ρ_{solid} (g/cm^3)	V_{tot} (cm^3)	I_{bulk}/I_{pore}	porosity (cm^3/g)	porosity[a] (cm^3/g)
CPG 81	0.71	2.23	1.21	1.84	0.44	0.49
silica gel 100	0.39	2.23	1.07	1.40	0.95	0.9−1.2

[a] Announced by the manufacturer.

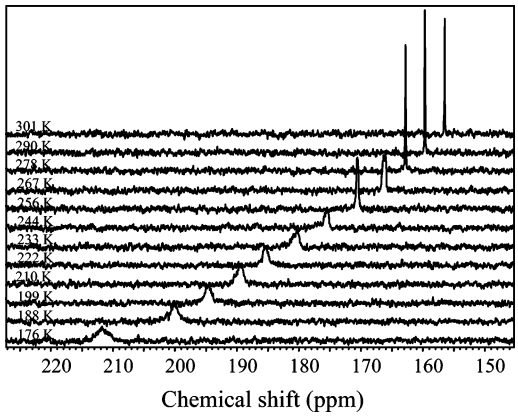

Figure 7. ^{129}Xe NMR spectra of xenon gas dissolved in cyclohexane. The measurement temperatures are shown at the spectra.

V_{pore} can be considered to be very nearly temperature-independent, the change is probably due to a difference in the solubilities of xenon in confined and bulk acetonitrile. Therefore, accurate porosity measurements require information about these solubility differences. Another choice is to add a coefficient before the ratio I_{bulk}/I_{pore} in eq 5 that could be calibrated by known reference samples.

4. Cyclohexane as a Medium

4.1. Xenon in Bulk Cyclohexane. At low temperatures, bulk cyclohexane forms a rigid monoclinic crystal. It undergoes a solid−solid phase transition to a plastic cubic phase at 186 K. In the plastic phase, the centers of the molecules are arranged in a regular cubic lattice with a positional long range order, but the molecules are more or less free to rotate.[14] The melting point (the plastic−liquid transition point) of cyclohexane is 280 K.[15]

The ^{129}Xe NMR spectra of xenon gas dissolved in pure cyclohexane measured at different temperatures (176−301 K) are shown in Figure 7. Contrary to the spectra from acetonitrile, the signal of dissolved xenon can also be observed in the solid phases. The integral of the signal decreases slightly in the liquid−plastic and plastic−solid transitions, indicating small reductions in solubility. In the liquid phase, the chemical shift of the signal increases linearly with decreasing temperature and the linear evolution continues also below the melting point, with a slightly different slope. No abrupt jump in the chemical shift is observed in the liquid−plastic transition. Near the plastic−solid transition point, the chemical shift begins to increase rapidly. Because of the high xenon pressure in the sample (5 atm), the temperatures of the transition points are a few degrees lower than those in normal conditions.

To analyze the NMR data, it is important for one to know how the density of cyclohexane depends on temperature. In the liquid phase, this dependence is well-known.[16] However, only three density−temperature data points are available in the solid phases (from the reported crystal structures). As a matter of fact, additional data points can be obtained from the results of the present NMR data. This is based on the fact that the chemical shift of a dissolved noble gas (relative to its gas phase signal at zero pressure) is directly proportional to the density (ρ) of the solvent.[17] In an isotropic environment, like in the liquid and cubic plastic crystal of cyclohexane, the chemical shift of a noble gas atom at temperature T can be written as[18]

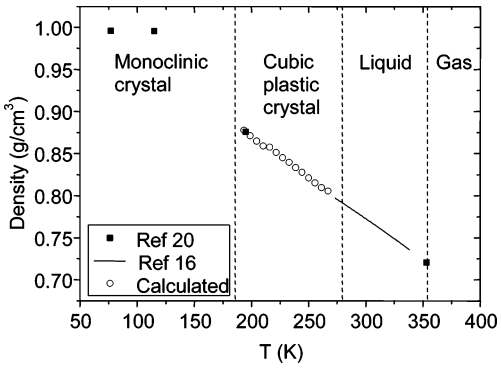

Figure 8. Density and phases of cyclohexane as a function of temperature. The values denoted by open circles are calculated from the chemical shifts of dissolved xenon (see text). The other values are measured densities or they have been calculated from the crystal structure.[16,20]

$$\delta = \rho(T)\,\delta_0[1 - \epsilon(T - T_0)], \tag{6}$$

where δ_0 and ϵ are constants, and T_0 is the reference temperature.

To observe the purely microscopic part of the medium-induced chemical shift, the bulk susceptibility correction is applied. For a long, cylindrical, isotropic sample with the tube axis parallel with the external magnetic field this contribution is[19]

$$\delta_b = \frac{\chi\rho}{3M}. \tag{7}$$

The magnetic susceptibility, χ, and molar mass, M, of cyclohexane are -6.78×10^{-5} cm^3/mol[20] and 84.2 g/mol, respectively. In view of the very nearly linear dependence of the chemical shift of xenon on temperature in the liquid and plastic phases, the density, ρ, in eq 7 is also taken to be a linear function of temperature. The resulting bulk susceptibility corrections are of the order of 0.2 ppm.

The values of parameters δ_0 and ϵ were solved by substituting the known densities and corrected chemical shifts determined at two different temperatures, 195 and 273 K, into eq 6. Using the reference temperature $T_0 = 273$ K, the resulting values were $\delta_0 = 208.3$ ppm cm^3/g and $\epsilon = 1.19 \times 10^{-3}$ 1/K. With these parameters and measured chemical shifts, the densities of cyclohexane at the other temperatures in the plastic phase were calculated by using eq 6. The results are displayed in Figure 8. They show that the density increases linearly with decreasing temperature in the liquid and plastic phase alike, and it does not exhibit any discontinuity at the liquid−plastic transition. However, because of the different pressures, the exact values of the density may be slightly different in the actual samples containing porous materials.

4.2. Xenon in Confined Cyclohexane. The ^{129}Xe NMR spectra of xenon dissolved in a sample containing silica gel 100 and cyclohexane as a medium are shown in Figure 9, and the chemical shifts of the signals as a function of temperature are seen in Figure 10. Signal A arises from the inner xenon thermometer, which is a capillary tube in the middle of the sample tube containing ethyl bromide and xenon gas.[21] At the highest temperatures, the spectra contain the signals of xenon dissolved in bulk and confined cyclohexane (denoted by B and

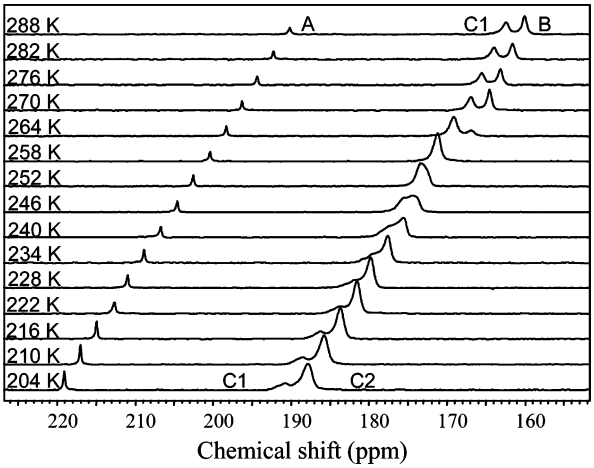

Figure 9. ^{129}Xe NMR spectra of the sample containing silica gel 100, cyclohexane, and xenon. The measurement temperatures are shown at the spectra.

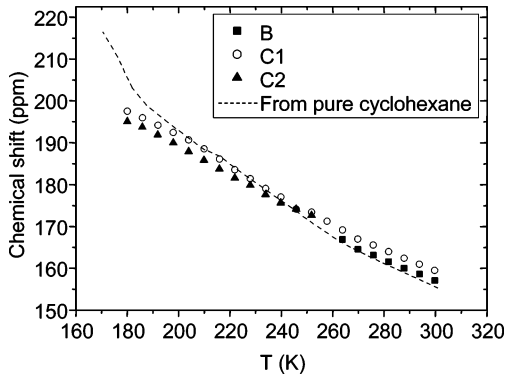

Figure 10. ^{129}Xe chemical shifts of the xenon dissolved in the sample containing silica gel 100 and cyclohexane. The shifts measured from the sample containing only cyclohexane and xenon are shown by the dashed line.

C1, respectively), as in the case of acetonitrile. Below the liquid-plastic transition point of the bulk medium, signal B vanishes gradually and the intensity of signal C1 increases, as the dissolved xenon atoms move from the bulk plastic phase to the confined liquid phase. Again, the phase transition point is lowered because of the high xenon pressure (~3.5 atm) and the particles of porous materials.

From the Gibbs−Thompson equation (eq 1) together with the values $k_p = 724$ KÅ (determined for cyclohexane by Aksnes and Kimtys[22]) and $R_p = 31.9$ Å (determined for silica gel 100 in the present work by the NMR cryoporometry), the liquid-plastic transition point depression can be estimated to be 23 K. Therefore, the transition point of confined cyclohexane should be a few degrees below 257 K. Indeed, a new signal, C2, located on the right shoulder of signal C1, emerges at about 252 K. Although the intensity of this signal increases with lowering temperature, the intensity of signal C1 decreases. An obvious interpretation is that signals C1 and C2 arise from xenon in the liquid and plastic phases of the confined cyclohexane, respectively.

In striking contrast to the samples containing acetonitrile as a medium, signal D is entirely absent in the spectra from the cyclohexane samples. This is due to the very different behavior of the density of acetonitrile and cyclohexane at the liquid−solid transition point. Although the density of acetonitrile increases abruptly about 20% at the freezing transition, there is no discontinuity at the liquid−plastic transition of cyclohexane. Hence, no cavities are built up inside the pores filled by

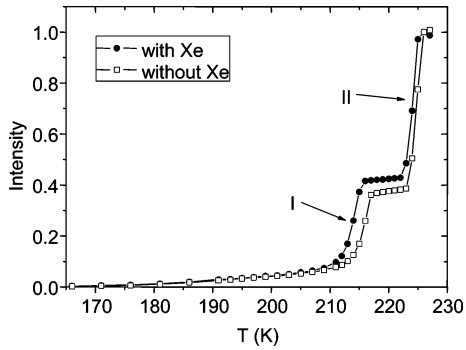

Figure 11. Relative intensity of the ^{1}H NMR signal of acetonitrile from the samples with and without xenon gas.

cyclohexane upon the liquid−solid transition. Because signal D originates from the xenon atoms sited in these cavities, it is absent in the cyclohexane samples.

Also, when cyclohexane is used as a medium, the difference of the chemical shifts of the signals from the confined and bulk liquids (C1 and B), $\delta_{C1} - \delta_B = \Delta\delta_{CB}$, depends on the pore radius. The differences determined at 300 K from samples containing three different silica gels are shown in Figure 5. In the restricted range of the pore radii of these samples, the relation between R_p and $\Delta\delta_{CB}$ can be modeled by the linear function

$$R_p = x + y\Delta\delta_{CB} \tag{8}$$

A least-squares refinement of parameters x and y resulted in the values $x = 37.48$ Å and $y = -2.604$ Å/ppm.

5. Influence of Xenon Gas on the Melting Points

The melting points of both bulk and confined acetonitrile can be determined from ^{129}Xe NMR spectra measured at different temperatures from xenon dissolved in samples containing porous material. These melting points, together with the Gibbs−Thompson equation (eq 1), provide one possibility for determining the size of the pores, as was shown in our previous work.[2]

Xenon gas dissolved in a medium can be considered as an impurity. In addition, it increases the pressure in the sample tube. Both things lower the melting point of bulk and confined medium. Because this phenomenon may affect the pore sizes calculated by the Gibbs−Thompson equation, it has been studied in the present work by means of the NMR cryoporometry method described in detail by Aksnes et al.[6] Two samples containing CPG 81 material immersed in acetonitrile were used, one containing about 3.5 atm xenon gas, the other without xenon. The intensity of the ^{1}H NMR signal of liquid acetonitrile measured from these samples as a function of temperature is shown in Figure 11. At the lowest temperatures, almost all of the acetonitrile has frozen and the intensity is very small. The intensity increases with increasing temperature (in region I) until all of the confined acetonitrile has melted. The second increase in the intensity (in region II) is due to the melting of the bulk acetonitrile. The presence of xenon lowers the former and latter melting points by about 1−2 K and 0.5−1 K, respectively, resulting in a slight increase in their difference. This has to be taken into account when the pore sizes are determined by utilizing the Gibbs−Thompson equation.

6. Hysteresis

To obtain reliable results, it is important for one to know if any hysteresis phenomena occur in the samples, that is, if the states of the samples depend on their history. In the present

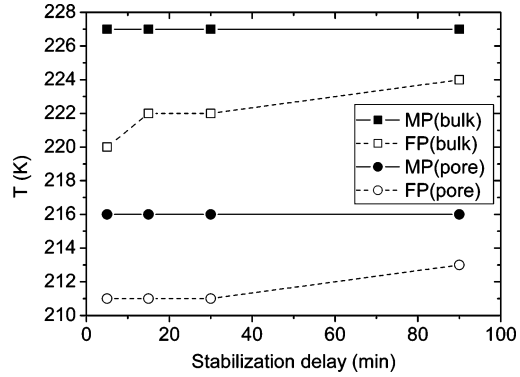

Figure 12. Melting points (MP) and freezing points (FP) of bulk and confined acetonitrile in a sample containing CPG 81 as a function of the temperature stabilization delay.

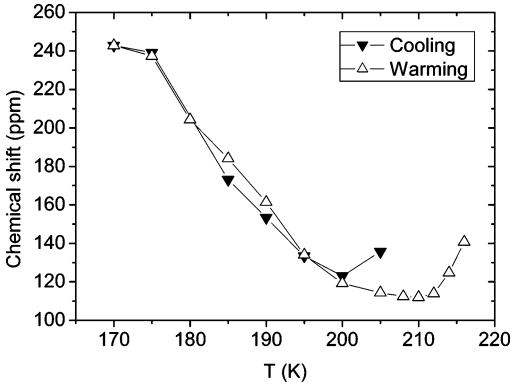

Figure 13. Chemical shift of signal D measured from the sample containing silica gel 100, acetonitrile, and xenon as a function of temperature during cooling and warming periods.

study, that was investigated in a sample containing CPG 81, acetonitrile, and xenon gas. ^{129}Xe spectra were measured from the sample at different temperatures first from 240 K down to 200 K and immediately thereafter back from 200 K up to 240 K using four different temperature stabilization times (5, 15, 30, and 90 min). The temperature step between successive measurements was 1−5 K, and the steps were set to the smallest values (1−2 K) around the phase transition temperatures.

The melting and freezing temperatures of the bulk and confined acetonitrile (determined from the disappearance or reappearance of signals B and D) are shown in Figure 12. Because the melting and freezing temperatures are different, hysteresis occurs in the sample. Figure 12 shows that the melting temperatures of both the bulk and confined acetonitrile are independent of the temperature stabilization delay, and their difference is $\Delta T = 11$ K for all of the delays. Substitution of this ΔT into the Gibbs−Thompson eq 1 together with $k_p = 478$ KÅ results in the pore radius of 43.5 Å, in reasonable agreement with the nominal radius of 40.5 Å.

When the temperature is lowered, substantial supercooling of both the bulk and confined acetonitrile is observed. In the case of the shortest temperature stabilization delay (5 min), the freezing of the bulk and confined medium takes place 7 and 5 K below the corresponding melting points, respectively. In the case of the longest delay (90 min), both freezing point depressions are 3 K. Measurements from a sample containing silica gel 100 with the temperature stabilization delay of 15 min revealed a still greater supercooling effect of about 11 K for both bulk and confined medium. However, it has little or no effect on the *difference* of the freezing points of the bulk and confined acetonitrile. Nevertheless, it is better to avoid the supercooling effects by making the measurements from low to high temperatures.

The chemical shift of signal D in a cooling−warming cycle measured from the sample containing Silica gel 100 using a temperature stabilization time of 15 min is shown in Figure 13. During the cooling period, signal D appears at 205 K. First, the chemical shift of the signal decreases with lowering temperature, which indicates that the gas pockets inside the pores grow up gradually within the temperature range of about 5 K. The intensity of signal D increases gradually with lowering temperature, as, on one hand, the size of the pockets increases and, on the other hand, more pores freeze. At still lower temperatures, the chemical shift begins to increase rapidly because of the liquefaction of xenon. Around 175 K, the shift reaches the chemical shift of liquid xenon, when almost all of the xenon in the pockets is in liquid state.

During the warming period, no obvious hysteresis phenomena can be observed in the chemical shift of signal D until near the phase transition temperature. Because of the different phase transition points, signal D is detectable at much higher temperatures than those in the cooling period. At the highest temperatures, the chemical shift increases rapidly because the gas pockets inside the pores shrink down gradually. This temperature range is approximately as wide as that during the build up of the pockets in the cooling period.

Hysteresis in phase transitions of substances confined to porous materials have also been studied by ^{1}H NMR spectroscopy,[23] X-ray diffraction,[24] optical experiments,[25] static light scattering,[26] and heat capacity measurements,[27] among others. There are a variety of explanations of the hysteresis phenomenon in the literature.[26,28,29]

7. Conclusions

Our previous work[2] demonstrated that ^{129}Xe NMR of xenon dissolved in a medium confined to pores can be used for a detailed characterization of the properties of porous materials. In the present work, the possibilities and limitations of the method have been investigated by using a variety of porous materials with different pore sizes and two different media. The results can be summarized as follows.

When acetonitrile is used as a medium, there are three techniques for measuring the pore sizes: from the chemical shift of signal D, from the difference of the chemical shifts of signals C and B, and from the melting point depression.

The chemical shift of signal D, originating from the xenon atoms sited in small pockets built up inside the pores during the freezing transition, is highly sensitive to the pore size. After calibration, it can be used to measure mean pore radii ranging from about 20 Å up to micrometer scale. Because solid acetonitrile prevents xenon atoms from moving from one pore to another, the observed resonance frequency is characteristic of the corresponding pore size. Hence, the distribution of the frequencies of atoms in different pores (signal D) represents the pore size distribution, which can be extracted from the spectrum by using the correlation determined in the present work. However, the experiments show that when the pore diameter exceeds about 500 Å, the intrinsic line width of the signal becomes so large that it masks the effects of the pore size distribution. However, the liquefaction of xenon at the lowest temperatures complicates the determination of the pore size distribution when the diameters of the pores are smaller than ∼70 Å.

The difference of the chemical shifts of signals arising from xenon dissolved in bulk (signal B) and confined liquid (signal

C) makes it possible to measure the pore sizes of the smaller pores (diameter smaller than ~120 Å). These measurements can also be done at room temperature, when acetonitrile or cyclohexane is used as the medium. If the diffusion of xenon atoms in the medium is sufficiently slow, then the frequency distribution of the atoms in the confined medium can even reveal the pore size distribution.

Because the phase transitions of the bulk and confined medium are seen easily from the spectra, the pore sizes can also be estimated by the Gibbs−Thompson equation, if the influence of dissolved xenon on the transition points is taken into account.

Apart from the pore sizes, the spectra also contain information about porosity. Because the intensities of the signals of xenon dissolved into the bulk and confined liquid (signals B and C, respectively) are directly proportional to the volumes of the corresponding phases, the porosities can be calculated by means of the ratio of the two intensities. Naturally, this presumes that signals B and C do not merge together. In the case of acetonitrile, this condition becomes true when the pore diameter is smaller than ~120 Å.

These methods for the determination of the pore sizes and porosities of materials can be optimized by using a medium that is best suited for each problem. For example, when cyclohexane is used as the medium, the difference of the chemical shifts of signals B and C is somewhat more sensitive to the pore size than in the case of acetonitrile. However, then there is no signal D in the spectra because of the absence of discontinuous density change at the freezing point.

In conclusion, xenon porometry has been shown to be an efficient method for characterization of porous materials by simple and fast NMR measurements. In addition, the measurements reveal detailed information on the behavior of media in confinement.

Acknowledgment. We are grateful to the Academy of Finland (Grants 43979 and 203278) and Väisälä foundation (V.-V. T.) for financial support.

References and Notes

(1) Dullien, F. A. L. *Porous Media: Fluid Transport and Pore Structure*, 2nd ed.; Academic Press: San Diego, CA, 1992.
(2) Telkki, V.-V.; Lounila, J.; Jokisaari, J. *J. Phys. Chem. B* **2005**, *109*, 757. A patent application has been submitted, FI 20045381.
(3) Jokisaari, J. *Prog. NMR Spectrosc.* **1994**, *26*, 1.
(4) Jackson, C. L.; McKenna, G. B. *J. Chem. Phys.* **1990**, *93*, 9002.
(5) Strange, J. H.; Rahman, M. *Phys. Rev. Lett.* **1993**, *71*, 3589.
(6) Aksnes, D. W.; Førland, K.; Kimtys, L. *Phys. Chem. Chem. Phys.* **2001**, *3*, 3203.
(7) Jameson, A. K.; Jameson, C. J.; Gutowsky, H. S. *J. Chem. Phys.* **1970**, *53*, 2310.
(8) Jameson, C. J. *J. Chem. Phys.* **1974**, *63*, 5296.
(9) Dosseh, G.; Xia, Y.; Alba-Simionesco, C. *J. Phys. Chem B* **2003**, *107*, 6445.
(10) Abragam, A. *The Principles of Nuclear Magnetism*; Clarendon: Oxford, U.K., 1974.
(11) Pfeffer, M.; Luzt, O. *J. Magn. Reson., Ser. A* **1995**, *113*, 108.
(12) Weingärtner, H.; Haselmeier, R., Holz, M. *Chem. Phys. Lett.* **1992**, *195*, 596.
(13) Terskikh, V. V.; Moudrakovski, I. L.; Breeze, S. R.; Lang, S.; Ratcliffe, C. I.; Ripmeester, J. A.; Sayari, A. *Langmuir* **2002**, *18*, 5653.
(14) Bilgram, J. H. *Phys. Rep.* **1987**, *153*, 1.
(15) Kahn, R.; Fourme, R.; André, D.; Renaud, M. *Acta Crystallogr., Sect. B* **1973**, *29*, 131.
(16) West, C. J.; Dorsey, N. E. *International Critical Tables of Numerical Data*: *Physics, Chemistry and Technology*; McGraw-Hill: New York, 1928.
(17) Lounila, J.; Muenster, O.; Jokisaari, J. *J. Chem. Phys.* **1992**, *97*, 8977.
(18) Ylihautala, M.; Lounila, J.; Jokisaari, J. *J. Chem. Phys.* **1999**, *110*, 6381.
(19) Buckingham, A. D.; Burnell, E. E. *J. Am. Chem. Soc.* **1967**, *89*, 3341.
(20) Beilstein database, Beilstein Institute for the Advancement of Chemical Sciences.
(21) Saunavaara, J.; Jokisaari, J., to be published.
(22) Aksnes, D. W.; Kimtys, L. *Appl. Magn. Reson.* **2002**, *23*, 51.
(23) Overloop, K.; Van Gerven, L. *J. Magn. Reson. A* **1993**, *101*, 179.
(24) Morishige, K.; Kawano, K. *J. Chem. Phys.* **1998**, *110*, 4867.
(25) Awschalom, D. D.; Warnock, J. *Phys. Rev. B* **1987**, *35*, 6779.
(26) Grosse, K.; Ratke, L.; Feuerbacher, B. *Phys. Rev. B* **1997**, *55*, 2897.
(27) Molz, E.; Apollo, P. Y.; Chan, M. H. W.; Beamish, J. R. *Phys. Rev. B* **1993**, *48*, 5741.
(28) Brun, A.; Lallemand, A.; Quinson, J.-F.; Eyraud, C. *Thermochim. Acta* **1977**, *21*, 59.
(29) Vanfleet, R. R.; Mochel, J. M. *Surf. Sci.* **1995**, *341*, 40.